

World Journal of *Gastrointestinal Oncology*

World J Gastrointest Oncol 2024 June 15; 16(6): 2264-2866



EDITORIAL

- 2264 Dual primary gastric and colorectal cancer: The known hereditary causes and underlying mechanisms
Azer SA
- 2271 Application of *Fusobacterium nucleatum* as a biomarker in gastrointestinal malignancies
Yu LC, Li YP, Xin YM, Mao M, Pan YX, Qu YX, Luo ZD, Zhang Y, Zhang X
- 2284 T1 colorectal cancer management in the era of minimally invasive endoscopic resection
Jiang SX, Zarrin A, Shahidi N
- 2295 Mixed neuroendocrine and adenocarcinoma of gastrointestinal tract: A complex diagnosis and therapeutic challenge
Shenoy S
- 2300 Advancements in breath-based diagnostics for pancreatic cancer: Current insights and future perspectives
Tez M, Şahingöz E, Marth HF
- 2304 Colorectal cancer and dormant metastases: Put to sleep or destroy?
Senchukova MA

REVIEW

- 2318 Advances in targeted therapy for human epidermal growth factor receptor 2 positive in advanced gastric cancer
Jiang YK, Li W, Qiu YY, Yue M
- 2335 Research progress of ferroptosis regulating lipid peroxidation and metabolism in occurrence and development of primary liver cancer
Shu YJ, Lao B, Qiu YY
- 2350 Early monitoring values of oncogenic signalling molecules for hepatocellular carcinoma
Yao M, Fang RF, Xie Q, Xu M, Sai WL, Yao DF

MINIREVIEWS

- 2362 Therapeutic strategies targeting the epidermal growth factor receptor signaling pathway in metastatic colorectal cancer
Zhou Y, Wu S, Qu FJ
- 2380 Predicting the prognosis of hepatic arterial infusion chemotherapy in hepatocellular carcinoma
Wang QF, Li ZW, Zhou HF, Zhu KZ, Wang YJ, Wang YQ, Zhang YW

- 2394 Unraveling colorectal cancer prevention: The vitamin D - gut flora - immune system nexus

Zhan ZS, Zheng ZS, Shi J, Chen J, Wu SY, Zhang SY

ORIGINAL ARTICLE

Retrospective Cohort Study

- 2404 Unveiling the secrets of gastrointestinal mucous adenocarcinoma survival after surgery with artificial intelligence: A population-based study

Song J, Yan XX, Zhang FL, Lei YY, Ke ZY, Li F, Zhang K, He YQ, Li W, Li C, Pan YM

- 2419 Analysis of metabolic characteristics of metabolic syndrome in elderly patients with gastric cancer by non-targeted metabolomics

Zhang H, Shen WB, Chen L

Retrospective Study

- 2429 Predictive value of preoperative routine examination for the prognosis of patients with pT2N0M0 or pT3N0M0 colorectal cancer

Jing PF, Chen J, Yu ED, Miao CY

- 2439 Simplified liver imaging reporting and data system for the diagnosis of hepatocellular carcinoma on gadoteric acid-enhanced magnetic resonance imaging

Lyu R, Hu WJ, Wang D, Wang J, Ye YB, Jia KF

- 2449 Efficacy comparison of fruquintinib, regorafenib monotherapy or plus programmed death-1 inhibitors for microsatellite stable metastatic colorectal cancer

An TQ, Qiu H, Zhou QB, Zong H, Hu S, Lian YG, Zhao RH

- 2463 Development of a diagnostic nomogram for alpha-fetoprotein-negative hepatocellular carcinoma based on serological biomarkers

He L, Zhang C, Liu LL, Huang LP, Lu WJ, Zhang YY, Zou DY, Wang YF, Zhang Q, Yang XL

- 2476 Drug-eluting bead transarterial chemoembolization as neoadjuvant therapy pre-liver transplantation for advanced-stage hepatocellular carcinoma

Ye ZD, Zhuang L, Song MC, Yang Z, Zhang W, Zhang JF, Cao GH

- 2487 Association between *Helicobacter pylori* infection, mismatch repair, HER2 and tumor-infiltrating lymphocytes in gastric cancer

Castaneda CA, Castillo M, Bernabe LA, Sanchez J, Fassan M, Tello K, Wistuba II, Chavez Passiuri I, Ruiz E, Sanchez J, Barrera F, Valdivia D, Bazan Y, Abad-Licham M, Mengoa C, Fuentes H, Montenegro P, Poquioma E, Alatriza R, Flores CJ, Taxa L

- 2504 Impact of baseline hepatitis B virus viral load on the long-term prognosis of advanced hepatocellular carcinoma treated with immunotherapy

Pan D, Liu HN, Yao ZY, Chen XX, Li YQ, Zhu JJ, Han ZX, Qin XB

- 2520 Prediction of pathological complete response and prognosis in locally advanced rectal cancer

Xu YJ, Tao D, Qin SB, Xu XY, Yang KW, Xing ZX, Zhou JY, Jiao Y, Wang LL

Observational Study

- 2531** Extrahepatic cholestasis associated with paracoccidioidomycosis: Challenges in the differential diagnosis of biliopancreatic neoplasia
dos Santos JS, de Moura Arrais V, Rosseto Ferreira WJ, Ribeiro Correa Filho R, Brunaldi MO, Kemp R, Sankanrakutty AK, Elias Junior J, Bellissimo-Rodrigues F, Martinez R, Zangiacomini Martinez E, Ardengh JC

Clinical and Translational Research

- 2541** Development of a novel staging classification for Siewert II adenocarcinoma of the esophagogastric junction after neoadjuvant chemotherapy
Zhang J, Liu H, Yu H, Xu WX
- 2555** N6-methyladenosine methylation regulates the tumor microenvironment of Epstein-Barr virus-associated gastric cancer
Zhang Y, Zhou F, Zhang MY, Feng LN, Guan JL, Dong RN, Huang YJ, Xia SH, Liao JZ, Zhao K
- 2571** Hepatocellular carcinoma: An analysis of the expression status of stress granules and their prognostic value
Ren QS, Sun Q, Cheng SQ, Du LM, Guo PX
- 2592** Comprehensive analysis of clinical and biological value of *ING* family genes in liver cancer
Liu SC
- 2610** Epidemiology and prognostic nomogram for locally advanced gastric signet ring cell carcinoma: A population-based study
Yu ZH, Zhang LM, Dai ZQ, Zhang MN, Zheng SM
- 2631** Socioeconomic traits and the risk of Barrett's esophagus and gastroesophageal reflux disease: A Mendelian randomization study
Liu YX, Bin CL, Zhang L, Yang WT, An BP

Basic Study

- 2646** Complement factor I knockdown inhibits colon cancer development by affecting Wnt/ β -catenin/c-Myc signaling pathway and glycolysis
Du YJ, Jiang Y, Hou YM, Shi YB
- 2663** Fine-needle aspiration technique under endoscopic ultrasound guidance: A technical approach for RNA profiling of pancreatic neoplasms
Seyfedinova SS, Freylikhman OA, Sokolnikova PS, Samochernykh KA, Kostareva AA, Kalinina OV, Solonitsyn EG
- 2673** Comprehensive analysis of gene mutations and mismatch repair in Chinese colorectal cancer patients
Chen H, Jiang RY, Hua Z, Wang XW, Shi XL, Wang Y, Feng QQ, Luo J, Ning W, Shi YF, Zhang DK, Wang B, Jie JZ, Zhong DR
- 2683** Action of circulating and infiltrating B cells in the immune microenvironment of colorectal cancer by single-cell sequencing analysis
Zhang JP, Yan BZ, Liu J, Wang W

- 2697** Bidirectional effects of the tryptophan metabolite indole-3-acetaldehyde on colorectal cancer
Dai Z, Deng KL, Wang XM, Yang DX, Tang CL, Zhou YP
- 2716** Sm-like 5 knockdown inhibits proliferation and promotes apoptosis of colon cancer cells by upregulating p53, CDKN1A and TNFRSF10B
Mo CJ, Deng XY, Ma RL, Zhu K, Shi L, Li K
- 2727** Shi-pi-xiao-ji formula suppresses hepatocellular carcinoma by reducing cellular stiffness through upregulation of acetyl-coA acetyltransferase 1
Jian HY, Liang ZC, Wen H, Zhang Z, Zeng PH
- 2742** Aspirin suppresses hepatocellular carcinoma progression by inhibiting platelet activity
Zhao LJ, Wang ZY, Liu WT, Yu LL, Qi HN, Ren J, Zhang CG
- 2757** Circ_0004592: An auxiliary diagnostic biomarker for gastric cancer
Kong S, Xu YH, Zheng M, Ju SQ, Shi HC
- 2769** N-glycosylation of Wnt3 regulates the progression of hepatocellular carcinoma by affecting Wnt/ β -catenin signal pathway
Zhang XZ, Mo XC, Wang ZT, Sun R, Sun DQ

SYSTEMATIC REVIEWS

- 2781** Ferroptosis regulating lipid peroxidation metabolism in the occurrence and development of gastric cancer
Wang LM, Zhang WW, Qiu YY, Wang F

META-ANALYSIS

- 2793** Meta-analysis of transarterial chemoembolization combined with cryoablation *vs* transarterial chemoembolization alone for ≥ 5 cm hepatocellular carcinoma
Cheng JF, Sun QL, Tang L, Xu XJ, Huang XZ
- 2804** Dynamic contrast enhanced ultrasound in differential diagnosis of hepatocellular carcinoma: A systematic review and meta-analysis
Esposito G, Santini P, Termite F, Galasso L, Mignini I, Ainora ME, Gasbarrini A, Zocco MA
- 2816** Correlation analysis of interstitial maturity and prognosis of colorectal cancer: Meta-analysis
Liu ZJ, Zhang XW, Liu QQ, Wang SZ

SCIENTOMETRICS

- 2826** Visualization analysis of research hotspots and trends on gastrointestinal tumor organoids
Wang G, Liu T, He WT
- 2842** Trends and hotspots in gastrointestinal neoplasms risk assessment: A bibliometric analysis from 1984 to 2022
Fu QQ, Ma L, Niu XM, Zhao HX, Ge XH, Jin H, Yu DH, Yang S

LETTER TO THE EDITOR

- 2862** New perspectives in prognostication of hepatocellular carcinoma: The role and clinical implications of transient receptor potential family genes

Guan SH, Hu WJ, Wang XY, Gu YX, Zhou DH

RETRACTION NOTE

- 2865** Retraction note to: RNA-binding protein CPSF6 regulates IBSP to affect pyroptosis in gastric cancer

Wang XJ, Liu Y, Ke B, Zhang L, Liang H

ABOUT COVER

Editorial Board Member of *World Journal of Gastrointestinal Oncology*, Samy Azer, FACC, MD, PhD, Professor, Department of Medical Education, King Saud University College of Medicine, Riyadh 11461, Saudi Arabia. azer2000@optusnet.com.au

AIMS AND SCOPE

The primary aim of *World Journal of Gastrointestinal Oncology (WJGO, World J Gastrointest Oncol)* is to provide scholars and readers from various fields of gastrointestinal oncology with a platform to publish high-quality basic and clinical research articles and communicate their research findings online.

WJGO mainly publishes articles reporting research results and findings obtained in the field of gastrointestinal oncology and covering a wide range of topics including liver cell adenoma, gastric neoplasms, appendiceal neoplasms, biliary tract neoplasms, hepatocellular carcinoma, pancreatic carcinoma, cecal neoplasms, colonic neoplasms, colorectal neoplasms, duodenal neoplasms, esophageal neoplasms, gallbladder neoplasms, *etc.*

INDEXING/ABSTRACTING

The *WJGO* is now abstracted and indexed in PubMed, PubMed Central, Science Citation Index Expanded (SCIE, also known as SciSearch®), Journal Citation Reports/Science Edition, Scopus, Reference Citation Analysis, China Science and Technology Journal Database, and Superstar Journals Database. The 2023 edition of Journal Citation Reports® cites the 2022 impact factor (IF) for *WJGO* as 3.0; IF without journal self cites: 2.9; 5-year IF: 3.0; Journal Citation Indicator: 0.49; Ranking: 157 among 241 journals in oncology; Quartile category: Q3; Ranking: 58 among 93 journals in gastroenterology and hepatology; and Quartile category: Q3. The *WJGO*'s CiteScore for 2023 is 4.2 and Scopus CiteScore rank 2023: Gastroenterology is 80/167; Oncology is 196/404.

RESPONSIBLE EDITORS FOR THIS ISSUE

Production Editor: *Si Zhao*; Production Department Director: *Xiang Li*; Cover Editor: *Jia-Ru Fan*.

NAME OF JOURNAL

World Journal of Gastrointestinal Oncology

ISSN

ISSN 1948-5204 (online)

LAUNCH DATE

February 15, 2009

FREQUENCY

Monthly

EDITORS-IN-CHIEF

Monjur Ahmed, Florin Burada

EDITORIAL BOARD MEMBERS

<https://www.wjgnet.com/1948-5204/editorialboard.htm>

PUBLICATION DATE

June 15, 2024

COPYRIGHT

© 2024 Baishideng Publishing Group Inc

INSTRUCTIONS TO AUTHORS

<https://www.wjgnet.com/bpg/gerinfo/204>

GUIDELINES FOR ETHICS DOCUMENTS

<https://www.wjgnet.com/bpg/GerInfo/287>

GUIDELINES FOR NON-NATIVE SPEAKERS OF ENGLISH

<https://www.wjgnet.com/bpg/gerinfo/240>

PUBLICATION ETHICS

<https://www.wjgnet.com/bpg/GerInfo/288>

PUBLICATION MISCONDUCT

<https://www.wjgnet.com/bpg/gerinfo/208>

ARTICLE PROCESSING CHARGE

<https://www.wjgnet.com/bpg/gerinfo/242>

STEPS FOR SUBMITTING MANUSCRIPTS

<https://www.wjgnet.com/bpg/GerInfo/239>

ONLINE SUBMISSION

<https://www.f6publishing.com>



Basic Study

Shi-pi-xiao-ji formula suppresses hepatocellular carcinoma by reducing cellular stiffness through upregulation of acetyl-coA acetyltransferase 1

Hui-Ying Jian, Zi-Cheng Liang, Huan Wen, Zhen Zhang, Pu-Hua Zeng

Specialty type: Oncology

Provenance and peer review:

Unsolicited article; Externally peer reviewed.

Peer-review model: Single blind

Peer-review report's classification

Scientific Quality: Grade B, Grade B, Grade D, Grade D

Novelty: Grade A, Grade B, Grade C, Grade C

Creativity or Innovation: Grade A, Grade B, Grade C, Grade C

Scientific Significance: Grade B, Grade B, Grade C, Grade C

P-Reviewer: Hashimoto N, Japan; Watanabe T, Japan

Received: January 1, 2024

Revised: March 14, 2024

Accepted: April 23, 2024

Published online: June 15, 2024



Hui-Ying Jian, Zi-Cheng Liang, Graduate School, Hunan University of Chinese Medicine, Changsha 410208, Hunan Province, China

Huan Wen, Zhen Zhang, Pu-Hua Zeng, Hunan Provincial Hospital of Integrated Traditional Chinese and Western, Cancer Research Institute of Hunan Academy of Traditional Chinese Medicine, Hunan Academy of Chinese Medicine, Changsha 410006, Hunan Province, China

Co-corresponding authors: Zhen Zhang and Pu-Hua Zeng.

Corresponding author: Zhen Zhang, PhD, Doctor, Hunan Provincial Hospital of Integrated Traditional Chinese and Western, Cancer Research Institute of Hunan Academy of Traditional Chinese Medicine, Hunan Academy of Chinese Medicine, No. 58 Lushan Road, Changsha 410208, Hunan Province, China. zhangzhen@stu.hnuocm.edu.cn

Abstract

BACKGROUND

Previous studies have shown that the Shi-pi-xiao-ji (SPXJ) herbal decoction formula is effective in suppressing hepatocellular carcinoma (HCC), but the underlying mechanisms are not known. Therefore, this study investigated whether the antitumor effects of the SPXJ formula in treating HCC were mediated by acetyl-coA acetyltransferase 1 (ACAT1)-regulated cellular stiffness. Through a series of experiments, we concluded that SPXJ inhibits the progression of HCC by upregulating the expression level of ACAT1, lowering the level of cholesterol in the cell membrane, and altering the cellular stiffness, which provides a new idea for the research of traditional Chinese medicine against HCC.

AIM

To investigate the anti-tumor effects of the SPXJ formula on the malignant progression of HCC.

METHODS

HCC cells were cultured *in vitro* with SPXJ-containing serum prepared by injecting SPXJ formula into wild-type mice. The apoptotic rate and proliferative, invasive, and migratory abilities of control and SPXJ-treated HCC cells were compared. Atomic force microscopy was used to determine the cell surface morphology and the Young's modulus values of the control and SPXJ-treated

HCC cells. Plasma membrane cholesterol levels in HCC cells were detected using the Amplex Red cholesterol detection kit. ACAT1 protein levels were estimated using western blotting.

RESULTS

Compared with the vehicle group, SPXJ serum considerably reduced proliferation of HCC cells, increased stiffness and apoptosis of HCC cells, inhibited migration and invasion of HCC cells, decreased plasma membrane cholesterol levels, and upregulated ACAT1 protein levels. However, treatment of HCC cells with the water-soluble cholesterol promoted proliferation, migration, and invasion of HCC cells as well as decreased cell stiffness and plasma membrane cholesterol levels, but did not alter the apoptotic rate and ACAT1 protein expression levels compared with the vehicle control.

CONCLUSION

SPXJ formula inhibited proliferation, invasion, and migration of HCC cells by decreasing plasma membrane cholesterol levels and altering cellular stiffness through upregulation of ACAT1 protein expression.

Key Words: Shi-pi-xiao-ji formula; Hepatocellular carcinoma; Cellular stiffness; Plasma membrane cholesterol level; Acetyl-coA acetyltransferase 1

©The Author(s) 2024. Published by Baishideng Publishing Group Inc. All rights reserved.

Core Tip: Cellular stiffness is a key feature of cellular biomechanics and is determined by cholesterol levels in the plasma membrane. Traditional Chinese medicine (TCM) has demonstrated good anti-tumor effects, but underlying mechanisms are not well characterized. Herein, we investigated the effects of the Shi-pi-xiao-ji (SPXJ) herbal formula on the stiffness of hepatocellular carcinoma (HCC) cells. The SPXJ formula altered the stiffness of HCC cells by decreasing plasma membrane cholesterol levels through upregulation of acetyl-coA acetyltransferase 1. Subsequently, this inhibited the invasion and metastasis of HCC cells. Our study provides a scientific basis for the clinical use of TCM preparations in the treatment of HCC.

Citation: Jian HY, Liang ZC, Wen H, Zhang Z, Zeng PH. Shi-pi-xiao-ji formula suppresses hepatocellular carcinoma by reducing cellular stiffness through upregulation of acetyl-coA acetyltransferase 1. *World J Gastrointest Oncol* 2024; 16(6): 2727-2741

URL: <https://www.wjgnet.com/1948-5204/full/v16/i6/2727.htm>

DOI: <https://dx.doi.org/10.4251/wjgo.v16.i6.2727>

INTRODUCTION

Primary liver cancer (PLC) is a serious malignancy characterized by considerable histological and biological heterogeneity. According to the GLOBOCAN 2020 data, 910000 new cases of liver cancer and 830000 PLC-related deaths were reported worldwide[1]. PLC includes malignant tumors originating from hepatocytes or intrahepatic bile duct epithelial cells and is classified into the following three distinct pathological types: Hepatocellular carcinoma (HCC), intrahepatic cholangiocarcinoma (ICC), and combined HCC-ICC. HCC accounts for approximately 90% of the PLC cases. HCC is a significant global health challenge because of high prevalence and mortality rates, with an estimated 5-year survival rate of only 18%[2]. PLC is a highly prevalent malignant tumor in China with 45.3% of new cases and 47.1% deaths; moreover, PLC cases in China account for approximately half of the global incidence rates ($n = 389000$; fourth rank) and deaths ($n = 336000$; second rank)[3]. The median survival rate for liver cancer in China is approximately 23 months[4], and for advanced liver cancer, it is only 6 months[1,5]. Therefore, PLC is a remarkable burden for both patients and society. The treatment modalities for PLC vary depending on the disease stage. Available treatments include resection, radiofrequency ablation (RFA), interventional embolization, radiotherapy, systemic chemotherapy, as well as molecular targeted therapy and immunotherapy. However, PLC is associated with insidious onset, high malignancy, and rapid progression. Therefore, a considerable number of patients are diagnosed at intermediate or advanced stages of PLC and are not amenable to surgical intervention. Despite the approval and clinical testing of numerous drugs for advanced HCC, the median progression-free survival and overall survival rates remain disheartening[6]. The diagnostic and therapeutic landscape for PLC is therefore challenging because of the severity and diversity of the disease.

The rapid progression, recurrence, and metastatic potential of cancer is mainly influenced by the proliferative, invasive, and migratory abilities of the cancer cells. Therefore, suppressing proliferation, invasion, and migration of the HCC cells is a major strategy for inhibiting HCC progression. The migration and invasiveness of HCC cells involves changes in their biomechanical properties to facilitate intricate cellular movements and deformations. Cellular biomechanics plays a pivotal role in the behavior of cancer cells. Cellular stiffness is a key feature that defines the biomechanical properties of cancer cells. Cellular stiffness is intricately related with the motility and metastatic potential of cancer cells[7-9]. The cholesterol concentration in the cell membrane is one of the main determinants of cellular stiffness. Depletion of cholesterol levels in the cell membrane of tumor cells is associated with increased cellular stiffness

[10]. Acetyl-coA acetyltransferase 1 (ACAT1) (also named acyl-coenzyme A: Cholesterol acyltransferase) is an enzyme that transfers long-chain fatty acids to cholesterol to form cholesteryl esters, which subsequently coalesce and form cytosolic lipid droplets[11]. Therefore, ACAT1 regulates the cholesterol composition of the cell membrane.

The SPXJ formula contains 15 herbs, namely, *Hedysarum multijugum* Maxi. (Huangqi), *Panax Ginseng* C. A. Mey. (Renshen), *Poria Cocos* (Schw.) Wolf. (Fuling), *Fructus Ligustri Lucidi* (Nvzhenzi), *Epimrdii Herba* (Yinyanghuo), *Salviae Chinensis Herba* (Shijianchuan), *Persicae Semen* (Taoren), *Eupolyphaga steleophaga* (Tubeimu), *Akebiae Frucyus* (Yuzhizi), *Curcumae Radix* (Yujin), *Pinelliae rhizoma praeparatum* (Fabanxia), *Scutellariae Barbatae Herba* (Banzhilian), *Solanum Nigrum* Linn. (Longkui), *Gecko* (Bihu), *Gleditsiae Spina* (Zaojiaoci). SPXJ formula is rich in ginsenosides[12,13], polysaccharides[14, 15], curcumin[16-18], and various other anti-tumor active ingredients. A previous study reported that the SPXJ formula suppressed the growth and progression of HCC cells[19-21], specifically by suppressing HepG2 cells[22]. Furthermore, individual herbs used in the preparation of SPXJ formula regulate energy metabolism and apoptosis in HCC cells. However, the specific effects of these components on the biomechanical properties of HCC cells are unclear.

In this study, we investigated whether the anti-tumor effects of the SPXJ formula in the HCC were mediated by ACAT1-regulated alterations in plasma membrane cholesterol levels and cellular stiffness. The main goal was to establish a scientific basis for the use of traditional Chinese medicine (TCM) formulas in the treatment of PLC patients.

MATERIALS AND METHODS

Materials and antibodies

Methyl- β -cyclodextrin (M β CD, Cat. No. GC32697) was purchased from Good Laboratory Practice Bioscience (Montclair, United States). Water-soluble cholesterol (Chol, Cat. No. SLCP6290) was purchased from Sigma-Aldrich (St. Louis, MO). Dulbecco's modified eagle medium (DMEM, Cat. No. PM15210), phosphate-buffered saline (PBS, Cat. No. PB180327), fetal bovine serum (FBS, Cat. No. 164210), penicillin-streptomycin solution (Cat. No. PB180120) were purchased from Procell Life Science & Technology Co., Ltd. (Wuhan, China). Trypsin (0.25%) was purchased from ECTOP. Matrigel (Cat. No. 356234) was purchased from Corning (New York, United States). Amplex red cholesterol assay kit (Cat. No. 2649096) was purchased from ThermoFisher Scientific (Massachusetts, United States). RIPA lysis buffer (Strong) (Cat. No. CW2333) was purchased from CWBIO (Beijing, China). BCA protein concentration measurement Kit (Cat. No. P0010) was purchased from Beyotime Biotechnology Co., Ltd. (Shanghai, China). ACAT1 polyclonal antibody (Cat. No. GB112323), Recombinant anti - beta actin antibody (Cat. No. GB15003), HRP-conjugated goat anti-rabbit IgG (H + L) (Cat. No. GB23303) were purchased from Servicebio Technology Co., Ltd. (Wuhan, China).

Preparation for SPXJ formula

The SPXJ formula contained 15 herbs that were purchased from the Affiliated Hospital of Hunan Academy of Traditional Chinese Medicine (Changsha, China). The botanical composition of the SPXJ formula is listed in Table 1. The herbs were soaked in 5000 mL of water for 30 min at room temperature and then concentrated to 2000 mL by boiling for approximately 30 min. Then, the liquid herbal extract was harvested by filtration. The remaining herbal components were again extracted by boiling with water for another 30 min. Again, the liquid herbal extract was collected and combined with the previously collected liquid herbal extract. The liquid herbal extract was concentrated to 500 mL. The final preparation was sealed and stored at -20 °C. The SPXJ formula was maintained at 4 °C during use.

Animals

We purchased twenty 5-6 wk-old male SD rats (SPF grade; 180-220 g weight) from the Hunan Silaikejingda Experimental Animal Co., Ltd (Changsha, China) (quality certificate number: No. 4307272211011626852). The rats were housed in the Animal Experimental Center of the Hunan University of Chinese Medicine under a 12 h light/dark cycle with ad libitum access to food and water.

Preparation of SPXJ drug-containing serum

Based on the equivalent dose ratios converted to body surface area between humans and rats[23], according to the conversion of 3 times the daily dose of 70 kg adults, the drug group was given 37.26 g/kg/d by gavage with the Realizing the Spleen and Eliminating Accumulation Drink, and the control group was given 10 mL/kg/d by gavage with drinking water. The SPXJ group rats were administered with 2 mL of the prepared SPXJ formula *via* oral gavage once daily for 7 d. The control group was administered 2 mL of drinking water. One hour after the last intragastric administration, the rats were anesthetized with isoflurane, the abdominal aorta was cut, and the whole blood was collected. The blood was let to stand at room temperature for 1 h. Then, it was centrifuged at 3000 rpm for 15 min and the serum was harvested. The serum samples from each group were pooled, inactivated in a 56 °C water bath for 30 min, passed through a 0.22- μ m filter, and stored at -20 °C for later use.

Cell line and culture

The MHCC97H (SNL-401) and HepG2 (SNL-083) human HCC cell lines were purchased from the Sunncell Biotechnology Co., Ltd (Wuhan, China). The cells were cultured in DMEM medium supplemented with 10% FBS and 1% penicillin-streptomycin solution at 37 °C in a 5% CO₂ water jacket incubator (Thermo Fisher Scientific). The cells at 5th passage were used for all the experimental procedures.

Table 1 The composition of Shi-pi-xiao-ji formula

No.	Chinese Pinyin name	Latin scientific name	Plant parts	Amount (g)
1	Huangqi	<i>Hedysarum multijugum</i> Maxi.	Root	15
2	Renshen	<i>Panax Ginseng</i> C. A. Mey.	Root	5
3	Fuling	<i>Poria Cocos</i> (Schw.) Wolf.	Mycorrhizae	15
4	Nvzhenzi	<i>Fructus Ligustri Lucidi</i>	Fruit	9
5	Yinyanghuo	<i>Epmrdii Herba</i>	Leaf	5
6	Shijianchuan	<i>Salviae Chinensis Herba</i>	Leaf	15
7	Taoren	<i>Persicae Semen</i>	Seed	5
8	Tubiechong	<i>Eupolyphaga steleophaga</i>	Whole worm	5
9	Yuzhizi	<i>Akebiae Frucyus</i>	Fruit	9
10	Yujin	<i>Curcumae Radix</i>	Root	9
11	Fabanxia	<i>Pinelliae rhizoma praeparatum</i>	Root	5
12	Banzhilian	<i>Scutellariae Barbatae Herba</i>	Whole plant	15
13	Longkui	<i>Solanum Nigrum</i> Linn.	Whole plant	15
14	Bihu	<i>Gecko</i>	Whole worm	5
15	Zaojiaoci	<i>Gleditsiae Spina</i>	Thorn	6

Experimental groups and treatment

The logarithmically growing MHCC97H and HepG2 cells were divided into four distinct groups: Vehicle, SPXJ-serum, M β CD, and Chol. The cells in the SPXJ-serum group were cultured in medium containing 10% SPXJ drug-containing serum for 24 h or 48 h. The cells in the M β CD group were cultured in medium supplemented with 5 mmol/L M β CD for 24 h or 48 h. The cells in the Chol group were cultured in medium containing 1 mmol/L water-soluble cholesterol for 24 h or 48 h.

Colony formation assay

MHCC97H and HepG2 cells were seeded in 6-well plates at a density of 800 cells/well and cultured for 24 h. Subsequently, after removing the media, the cells were incubated with fresh growth medium containing different drugs and cultured for a week. The culture medium was then discarded. The cells were then fixed for 15 min with 1 mL of 4% paraformaldehyde. The colonies were stained with 1 mL of 1% crystal violet staining solution for 15 min at room temperature. Then, the wells were washed with running water and dried. The stained cells in the 6-well plates were photographed, and colonies with more than 50 cells were counted.

Wound healing assay

MHCC97H and HepG2 cells were seeded in 6-well plates at a density of 2×10^4 cells/well and cultured until a confluent monolayer was formed for 24 h. A clean scratch wound was then generated at the center of the monolayer in each well with a 200 μ L pipette. Subsequently, floating cells were removed by washing with PBS. Then, the monolayers of cells were incubated with fresh DMEM medium supplemented with 10% FBS and specific drugs (SPXJ-serum, M β CD, and Chol). The 6-well plates were incubated in a humidified incubator at 37 °C and 5% CO₂. The wounds were photographed at predetermined time intervals (24 h and 48 h). The migration rate was determined using the Image J software using the following formula: Migration (%) = (initial scratch width - final scratch width)/initial scratch width \times 100%.

Transwell assay

The upper chambers of the Transwell were coated with the diluted matrix Matrigel (1:7). MHCC97H and HepG2 cells were resuspended in serum-free DMEM medium and seeded into the upper chambers of the Transwell at a concentration of 1×10^4 cells per 100 μ L. The lower chambers of the Transwell were filled with DMEM medium supplemented with 10% FBS, which acted as a chemoattractant for the cells in the upper chamber. Subsequently, various drugs were added into the upper chambers. Transwell chambers were then incubated for 48 h in a humidified incubator maintained at 37 °C and 5% CO₂. The Matrigel and the non-invading cells on the upper surface of the membrane were gently removed using a cotton swab. The invading cells on the lower surface of the Transwell membrane were fixed, stained, visualized, and photographed under a light microscope. Image J software was used to count the number of invading cells in each group.

Cellular apoptosis assay

The apoptotic cells in each group were estimated using the apoptosis detection kit according to the manufacturer's instructions. MHCC97H and HepG2 cells were digested with EDTA-free trypsin, centrifuged at 1500 rpm for 5 min at 4

°C, and collected. The cells were washed twice with precooled PBS and centrifuged at 1500 rpm for 5 min. The cells [(1-5) × 10⁵ cells per group] were resuspended in 500 µL of 1 × binding buffer. Then, the cells were stained by adding 5 µL of Annexin V-FITC and 5 µL of propidium iodide (PI)-staining solution to the cell suspension, mixing gently, and incubating in the dark at room temperature for 10 min. The stained cells were then analyzed by flow cytometry within 1 h. The apoptosis rate was calculated with the following formula: (number of apoptotic cells/total number of cells observed) × 100%.

Atomic force microscope

MHCC97H and HepG2 cells were seeded at a density of 2 × 10⁴ cells/well in 24-well plates and cultured for 24 h to allow the formation of a confluent monolayer. The medium was then removed and various drugs were added. Subsequently, the cells were washed twice with PBS and fixed with 1% glutaraldehyde for 5 min. The fixed cells were washed twice with PBS. The Young's modulus values of the samples were determined under an atomic force microscope (AFM) after natural air drying by setting the spring constant of the cantilever at 0.5 N. The tips were cleaned with ethanol and UV light was used after each force map to remove the contaminations. The topography and Young's modulus images were recorded. Young's modulus maps were generated with a scan area of 10 micrometer × 10 micrometer with 30 × 30 force-indentation curves to determine the Young's modulus values for the cells from distinct groups.

Quantification of plasma membrane cholesterol levels

The total cellular cholesterol level was first quantified using the Amplex red cholesterol assay kit. MHCC97H and HepG2 cells were fixed with glutaraldehyde (0.1% in PBS) and the total cholesterol was extracted by sonication with the methanol/chloroform mixture (1:2, v/v). After removing the organic solvent under vacuum, the cholesterol level was quantified using the Amplex red cholesterol assay kit according to the manufacturer's instructions. To quantify the intracellular cholesterol levels, the fixed cancer cells were treated with cholesterol oxidase (2 U/mL in PBS) to oxidize the plasma membrane cholesterol before extraction. The plasma membrane cholesterol levels were calculated by subtracting the intracellular cholesterol levels from the total cellular cholesterol levels as previously described[24].

Western blotting

Total protein extracts were prepared from the MHCC97H and HepG2 cells by incubating with the RIPA lysis buffer at 4 °C for 30 min. The cell extracts were centrifuged at 14000 × g for 10 min at 4 °C and the supernatant was harvested. The protein concentration was measured by the BCA method. The protein concentrations of the samples were adjusted to 1.5 µg of total protein per microliter with the 5 × SDS loading buffer. The samples were denatured at 100 °C for 10 min. The samples were let to cool before use. SDS-PAGE electrophoresis was performed by loading 20 µL of each protein sample (30 µg protein per sample). The separated proteins were transferred from SDS polyacrylamide gels onto the nitrocellulose membranes. These membranes were blocked with 5% nonfat milk at room temperature for 1 h. Then, they were incubated overnight at 4 °C with primary antibodies such as anti-ACAT1 (1:1000), and anti-ACTIN (1:5000). The membranes were then washed three times with TBST (10 min each) and subsequently incubated with the HRP-conjugated secondary antibodies (1:10000) for 60 min. The membranes were washed thrice with TBST and the protein bands were visualized using the ECL detection system. The relative protein expression levels were then quantified using the Image J software.

Statistical analysis

Statistical analysis was performed using the SPSS 22.0 statistical software. The data with normal distribution were expressed as means ± SE with a sample size of *n* = 3. The differences between multiple groups were analyzed using the One-Way Analysis of Variance when the data satisfied the assumptions of normality and homogeneity of variances. Two-by-two comparisons between multiple groups were performed using the LSD-*t* test. However, if the assumption of homogeneity of variances was not met, the Welch test was used to compare the groups. *P* value < 0.05 was determined as statistically significant.

RESULTS

SPXJ-serum treatment induces remarkable changes in HCC cell morphology

The morphological changes in the vehicle- and drug-treated MHCC97H and HepG2 cells were analyzed using an inverted microscope (Figure 1). The cells in the vehicle group exhibited an epithelioid monolayer arrangement, and were characterized by irregular polygonal shapes, close adherence to the substrate, uniform size, and well-defined boundaries. In contrast, cells in the MβCD group were characterized by elongated or spindle-shaped morphology, uneven size, and indistinct margins in some cells (highlighted by orange arrows). The cells treated with the SPXJ-serum exhibited a more rounded shape and were accompanied by increased cellular debris in the culture fluid. The cells in the Chol group displayed irregular polygonal shape with clear and sharp edges. These observations suggested that treatment with the SPXJ formula induced remarkable changes in cell morphology.

SPXJ inhibits proliferation of HCC cells

Colony formation assay was performed to determine the effects of SPXJ on the proliferation of MHCC97H and HepG2 cells. In comparison with the vehicle group, the number and size of colonies were considerably reduced in the SPXJ-serum group (Figure 2). The number of colonies were considerably higher in the Chol group compared with the vehicle

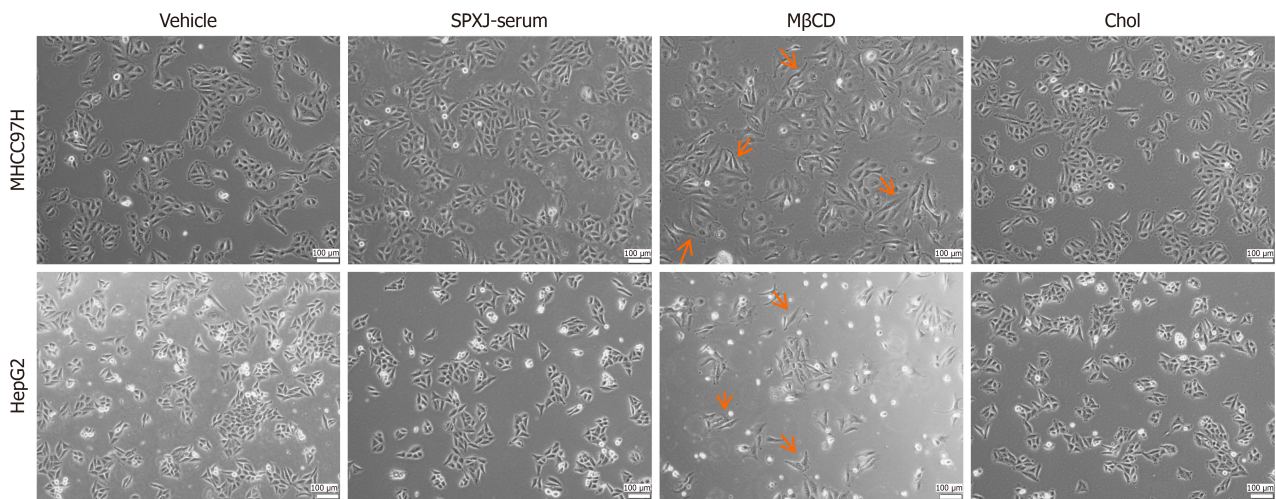


Figure 1 Representative images show the morphology of the vehicle, Shi-pi-xiao-ji-serum, methyl-β-cyclodextrin, and water-soluble cholesterol groups of MHCC97H and HepG2 cells. SPXJ: Shi-pi-xiao-ji; MβCD: Methyl-β-cyclodextrin; Chol: Water-soluble cholesterol.

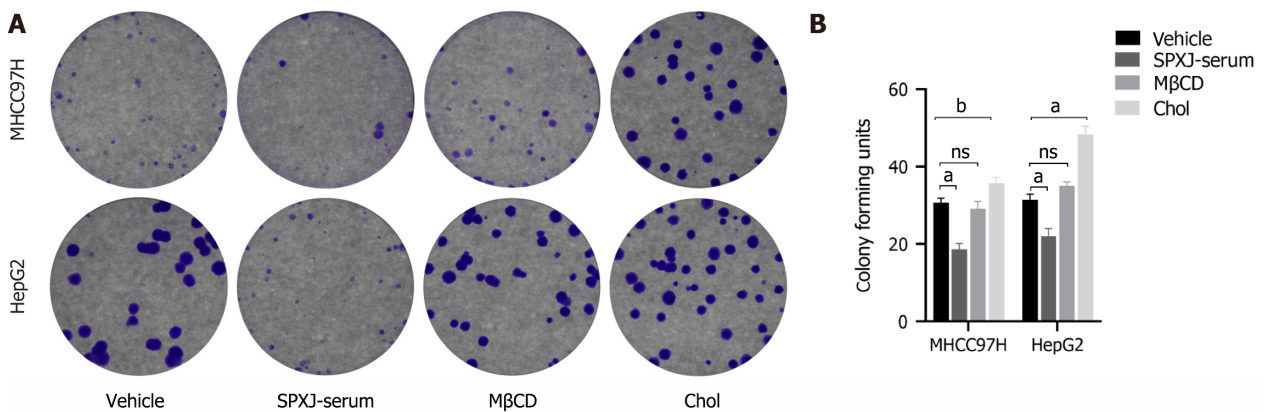


Figure 2 Representative images and statistical results of the colony formation assay in the vehicle, Shi-pi-xiao-ji-serum, methyl-β-cyclodextrin, and water-soluble cholesterol groups of MHCC97H and HepG2 cells. A: Representative images; B: Representative statistical results. The results are expressed as means ± SEM ($n = 3$). ^a $P < 0.05$, ^b $P < 0.01$, ns: $P > 0.05$. SPXJ: Shi-pi-xiao-ji; MβCD: Methyl-β-cyclodextrin; Chol: Water-soluble cholesterol.

group. However, the number of colonies in the MβCD group did not show statistically significant differences with the vehicle group. These data suggested that the SPXJ formula inhibited the proliferation of HCC cells.

SPXJ inhibits migration and invasion of HCC cells

The effects of the SPXJ formula on the migration and invasiveness of HCC cells were assessed using wounding healing and Transwell assays, respectively. The results of the wounding healing assay are shown in Figure 3A-D. At 24 h post-treatment, SPXJ-serum-treated MHCC97H cells did not show notable differences in the migration ability compared with the vehicle group, but the migration of SPXJ-serum treated HepG2 cells was considerably reduced. However, at 48 h, migration ability of the SPXJ-serum-treated MHCC97H and HepG2 cells was considerably reduced compared with the vehicle group. Furthermore, MβCD treatment remarkably reduced migration ability of both MHCC97H and HepG2 cells, whereas treatment with water-soluble cholesterol significantly increased the migration ability of MHCC97H and HepG2 cells. Moreover, the effects of different drug treatments were proportional to the duration of treatment. Transwell assay results are shown in Figure 3E and F. In comparison with the vehicle group, the invasiveness of SPXJ-serum- or MβCD-treated MHCC97H and HepG2 cells was significantly reduced. Conversely, the invasiveness of the water-soluble cholesterol-treated MHCC97H and HepG2 cells was significantly higher than the vehicle group. These findings demonstrated that the SPXJ formula inhibited *in vitro* migration and invasion of the MHCC97H and HepG2 cells.

SPXJ induces apoptosis of HCC cells

Flow cytometry analysis of annexin V/PI-stained cells was used to determine whether SPXJ formula induced HCC cell death (Figure 4). In comparison with the vehicle group, the proportion of apoptotic cells were significantly higher in the SPXJ-serum-treated MHCC97H cells (15.13% vs 35.31%). Furthermore, the proportion of apoptotic cells were significantly higher in the SPXJ-serum-treated HepG2 cells compared with the vehicle-treated HepG2 cells (19.37% vs 11.44%). The

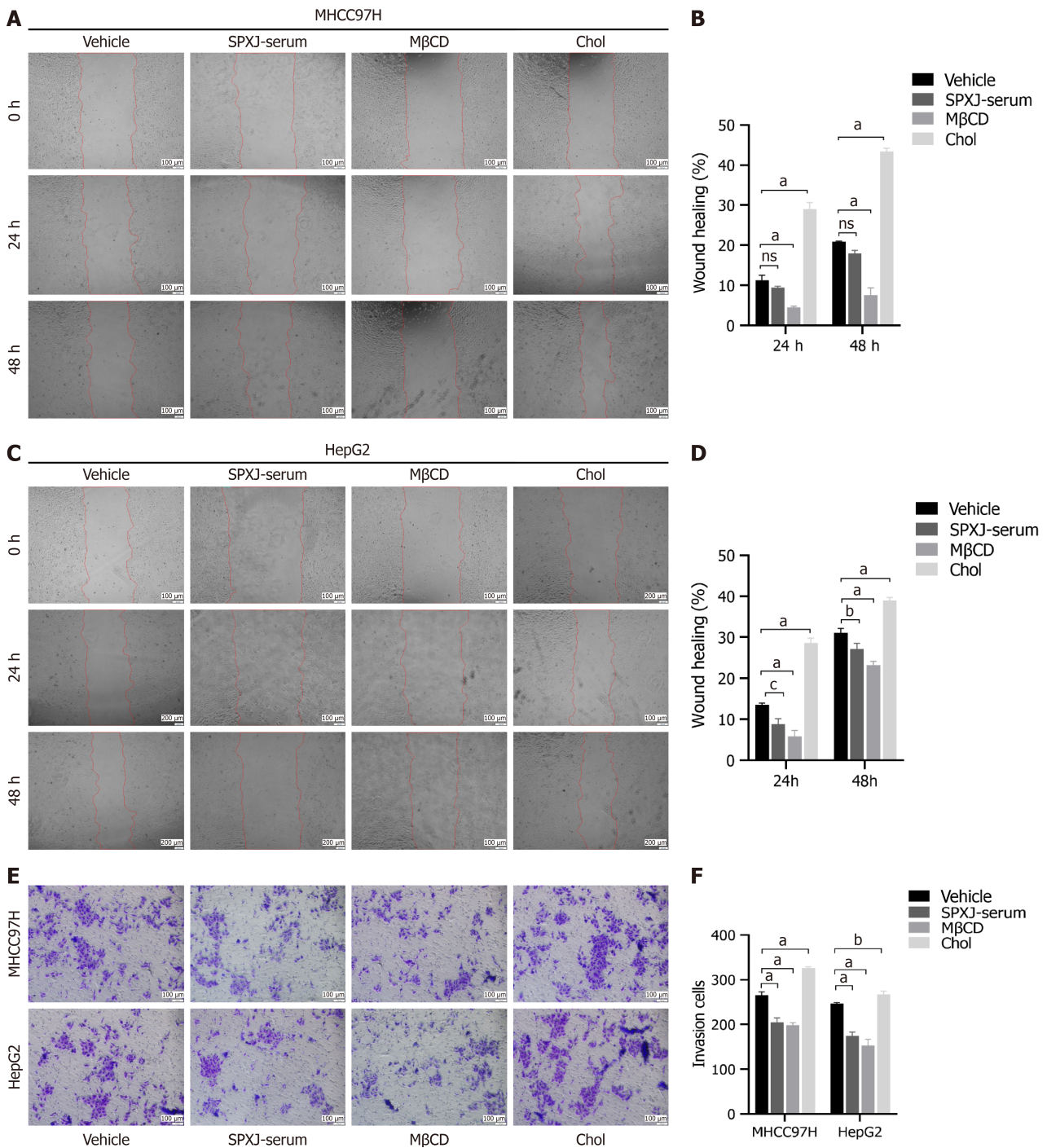


Figure 3 Representative images and statistical results of wounding healing and transwell assays. A and B: Representative images and statistical results of the wounding healing assay in the vehicle, Shi-pi-xiao-ji (SPXJ)-serum, methyl-β-cyclodextrin (MβCD), and water-soluble cholesterol (Chol) groups of MHCC97H cells; C and D: Representative images and statistical results of wounding healing assay in the vehicle, SPXJ-serum, MβCD, and Chol groups of HepG2 cells; E and F: Representative images and statistical results of the transwell assay in the vehicle, SPXJ-serum, MβCD, and Chol groups of hepatocellular carcinoma cells. The results are expressed as means ± SEM (n = 3). ^aP < 0.05, ^bP < 0.01, ^cP < 0.001, ns: P > 0.05. SPXJ: Shi-pi-xiao-ji; MβCD: Methyl-β-cyclodextrin; Chol: Water-soluble cholesterol.

proportion of apoptotic cells were significantly higher in the Chol group compared with the MβCD group. These findings demonstrated that treatment with the SPXJ-serum induced apoptosis in the HCC cells.

SPXJ decreases stiffness of HCC cells

The effects of the SPXJ formula on the stiffness of HCC cells was assessed using AFM. The representative AFM images and the Young’s modulus values for the HCC cells in all the groups are shown in Figure 5. In comparison with the vehicle group, the Young’s modulus values were significantly higher in the SPXJ-serum and MβCD group cells, but considerably decreased in the Chol group. The brightness in the AFM images corresponds with the height and the brightest area denotes the nucleus. The cell surface in the vehicle group displayed holes, regular and flat surface, and brighter

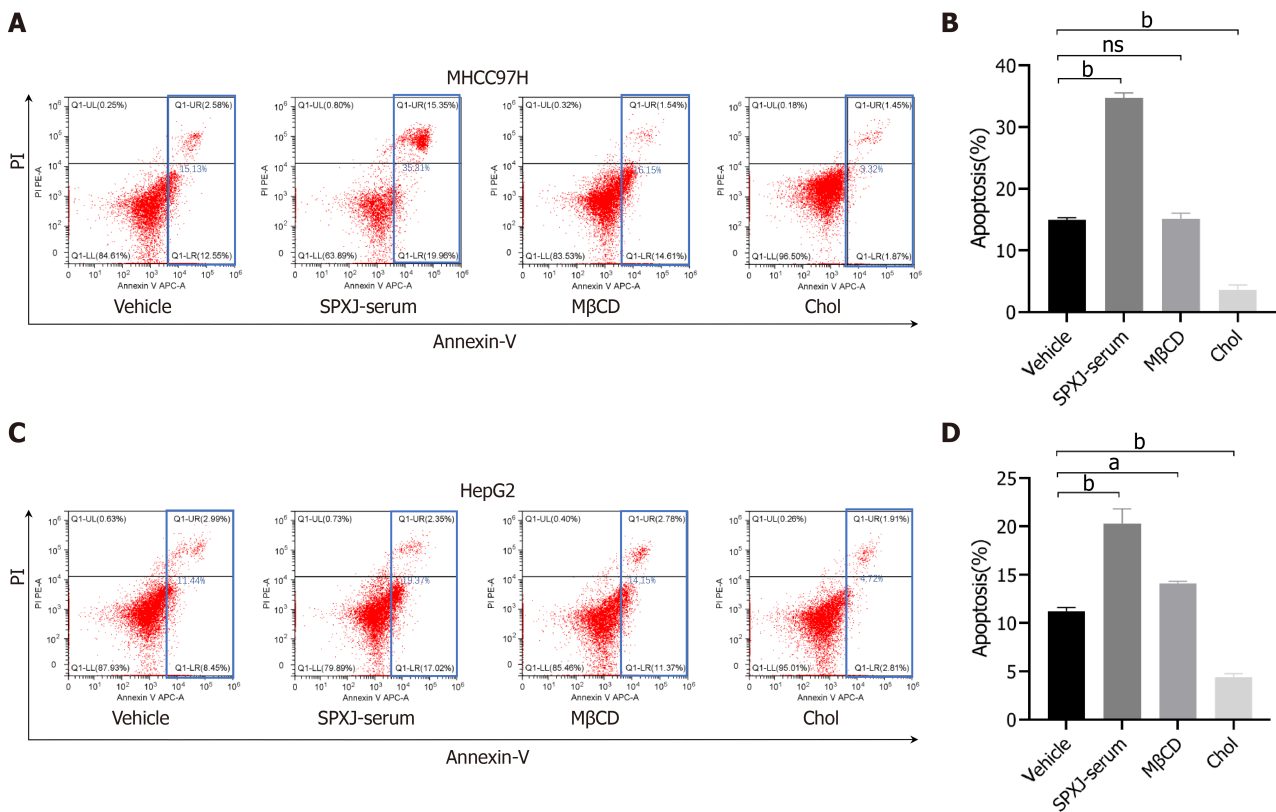


Figure 4 Flow cytometry results show the percentage of apoptotic hepatocellular carcinoma cells in the vehicle, Shi-pi-xiao-ji-serum, methyl-β-cyclodextrin, and water-soluble cholesterol groups of MHCC97H cells and HepG2 cells based on the annexin V/PI double-staining. A and B: Flow cytometry results show the percentage of apoptotic hepatocellular carcinoma (HCC) cells in the vehicle, Shi-pi-xiao-ji (SPXJ)-serum, methyl-β-cyclodextrin (MβCD), and water-soluble cholesterol (Chol) groups of MHCC97H cells based on the annexin V/PI double-staining; C and D: Flow cytometry results show the percentage of apoptotic HCC cells in the vehicle, SPXJ-serum, MβCD, and Chol groups of HepG2 cells based on the annexin V/PI double-staining. The results are expressed as means ± SEM (n = 3). ^aP < 0.01, ^bP < 0.001 and ns: P > 0.05. SPXJ: Shi-pi-xiao-ji; MβCD: Methyl-β-cyclodextrin; Chol: Water-soluble cholesterol; PI: Propidium iodide.

morphology. In comparison with the vehicle group and SPXJ-serum group, cells in the Chol group showed remarkable alterations in the cell surface morphology, including presence of large holes with varying depths on the cell surface (white arrow in the figure). Conversely, the MβCD group displayed a flat and smooth cell surface and did not show any obvious holes. These data suggested that SPXJ treatment altered the stiffness of the HCC cells.

SPXJ increases cellular stiffness by lowering plasma membrane cholesterol levels

Cholesterol-rich domains in the cell membranes regulate cellular stiffness. Therefore, we analyzed the effects of SPXJ-serum treatment on the cholesterol levels in the plasma membrane of the HCC cells. Amplex red cholesterol assay results are shown in Figure 6. SPXJ-serum and Chol groups showed significantly higher cholesterol levels in the plasma membrane of the HCC cells compared with the vehicle group, but the levels of plasma membrane cholesterol were significantly lower in the MβCD group. This demonstrated that SPXJ increased stiffness in the HCC cells by decreasing plasma membrane cholesterol levels.

SPXJ reduces plasma membrane cholesterol levels by increasing ACAT1 expression levels

ACAT1 is an enzyme that regulates formation of cholesteryl esters by transferring a long-chain fatty acid to cholesterol. Thus, ACAT1 regulates the levels of cholesterol in the cell membrane. Therefore, we performed western blotting to determine if the SPXJ formula decreased the stiffness of HCC cells by increasing ACAT1 protein expression levels. Western blotting results demonstrated that treatment with SPXJ-serum significantly upregulated ACAT1 protein levels while concurrently decreasing cholesterol levels in the plasma membrane (Figure 7). This, in turn, increased the stiffness of HCC cells and inhibited their migration and invasion. However, treatment of HCC cells with the cholesterol-depleting agent MβCD or water-soluble cholesterol did not show any statistically significant changes on the ACAT1 protein expression levels.

DISCUSSION

PLC is the fourth leading cause of cancer-related deaths globally[25,26]. Therefore, PLC is a considerable public health

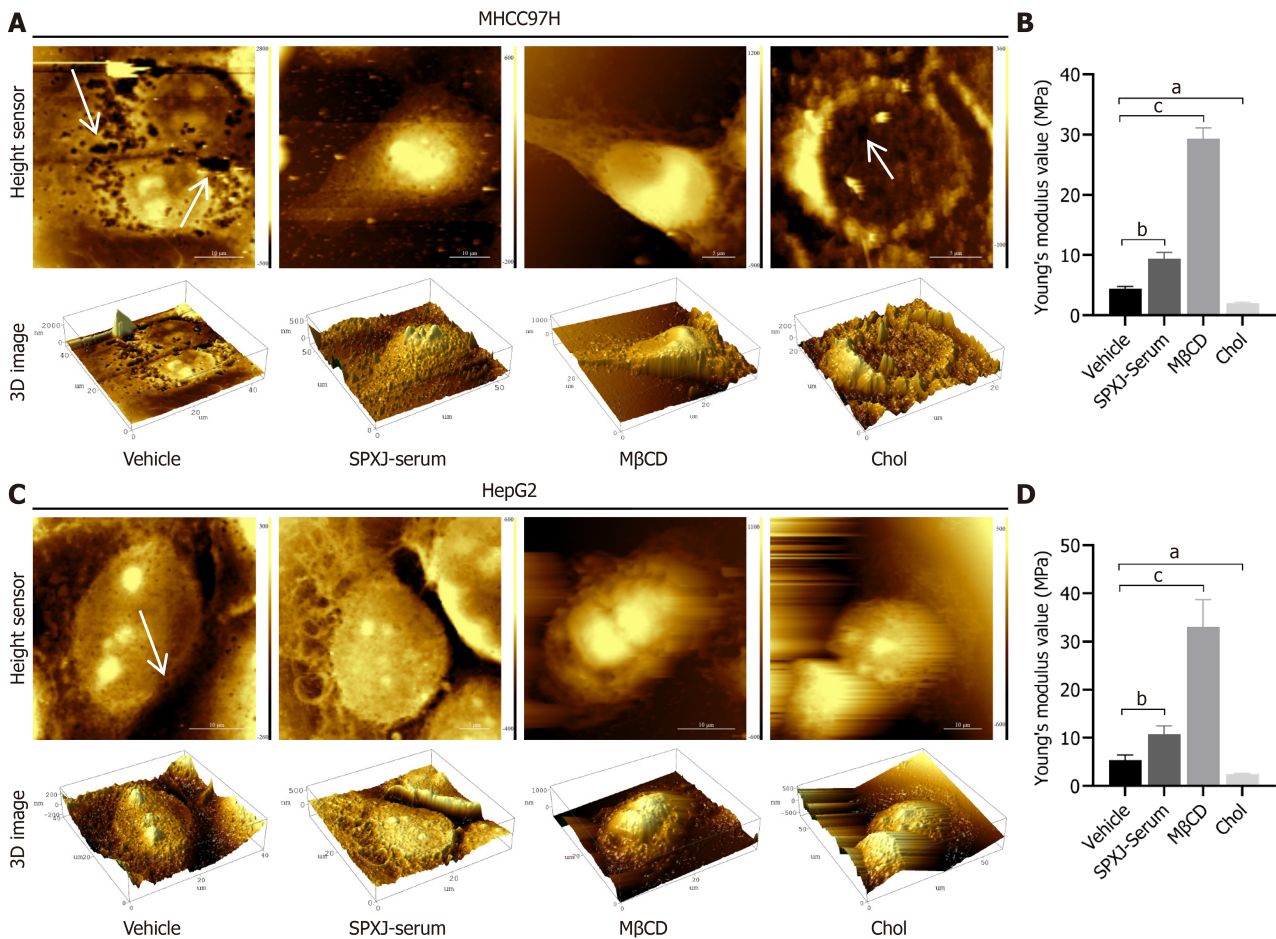


Figure 5 Representative atomic force microscope images and Young's modulus values. A and B: Representative atomic force microscope (AFM) images (A) and Young's modulus values (B) of MHCC97H cells in the vehicle, Shi-pi-xiao-ji (SPXJ)-serum, methyl-β-cyclodextrin (MβCD), and water-soluble cholesterol (Chol) groups; C and D: Representative AFM images (C) and Young's modulus values (D) of HepG2 cells in the vehicle, SPXJ-serum, MβCD, and Chol groups. The results are expressed as means ± SEM (n = 3). ^aP < 0.05, ^bP < 0.01, ^cP < 0.001. SPXJ: Shi-pi-xiao-ji; MβCD: Methyl-β-cyclodextrin; Chol: Water-soluble cholesterol.

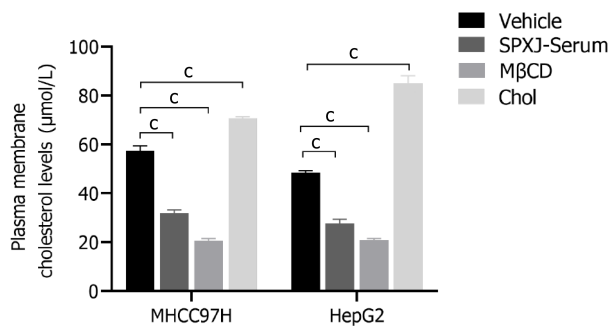


Figure 6 The total plasma membrane cholesterol levels in the vehicle, Shi-pi-xiao-ji-serum, methyl-β-cyclodextrin, and water-soluble cholesterol groups of MHCC97H and HepG2 cells. The results are expressed as means ± SEM (n = 3). ^cP < 0.001. SPXJ: Shi-pi-xiao-ji; MβCD: Methyl-β-cyclodextrin; Chol: Water-soluble cholesterol.

challenge. The morbidity and mortality rates of patients with PLC have increased considerably over the past decades. According to the World Health Organization data, an estimated 1276679 individuals are estimated to die because of liver cancer in the year 2040. The incidence and mortality rates of PLC show substantial regional variations with countries in East Asia and sub-Saharan Africa reporting the highest incidence rates. The incidence rate of PLC is high in China with an estimated 18.3 cases per 100000 individuals[27,28]. Patients with early or intermediate-stage HCC are treated with localized locoregional therapies, including RFA, resection, transplantation, percutaneous ethanol injection, or transcatheter arterial chemoembolization. Furthermore, patients with HCC can be treated with systemic approaches such as chemotherapy, molecular targeted therapy, and immunotherapy. Despite promising developments in drug discovery, the prognosis of HCC remains poor. The median progression-free survival and overall survival rates of intermediate and

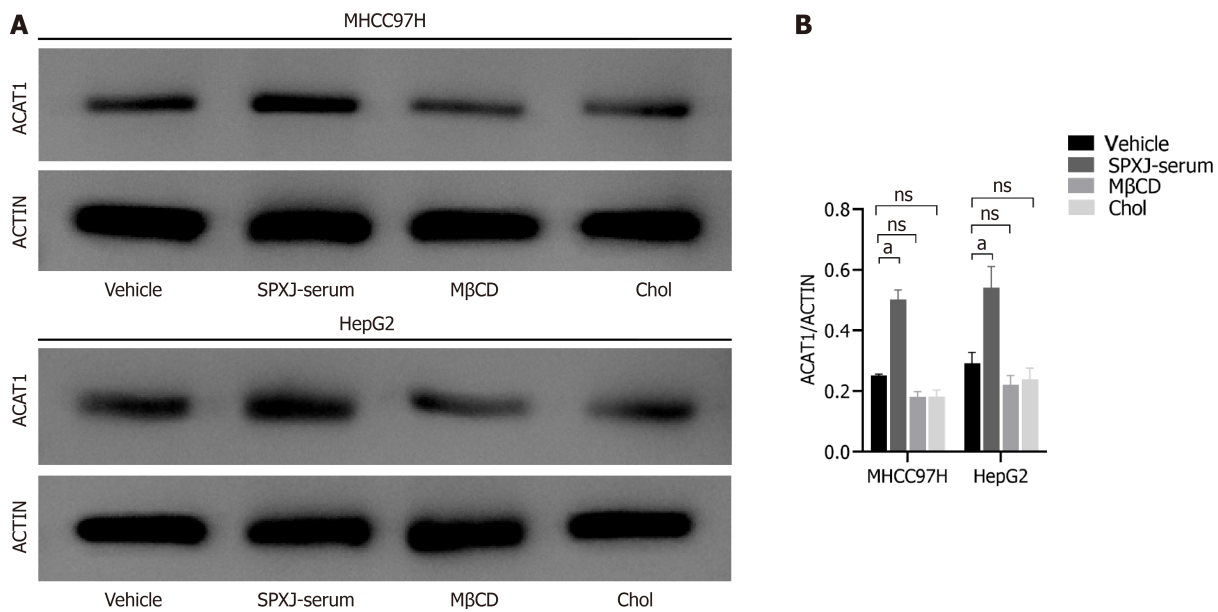


Figure 7 Western blot analysis of acetyl-coA acetyltransferase 1 protein expression levels. A: Representative image shows the expression of acetyl-coA acetyltransferase 1 (ACAT1) protein in vehicle, Shi-pi-xiao-ji (SPXJ)-serum, methyl-β-cyclodextrin (MβCD), and water-soluble cholesterol (Chol) groups of MHCC97H and HepG2 cells. Actin was used as loading control; B: Histogram plots show the relative expression levels of ACAT1 protein in the vehicle, SPXJ-serum, MβCD, and Chol groups of MHCC97H and HepG2 cells. The results are expressed as means ± SEM (n= 3). ^aP < 0.01, ns: P > 0.05. SPXJ: Shi-pi-xiao-ji; MβCD: Methyl-β-cyclodextrin; Chol: Water-soluble cholesterol; ACAT1: Acetyl-coA acetyltransferase 1.

advanced stage in patients with HCC remain considerably low. The diagnosis and treatment of PLC, especially HCC, remains a substantial challenge.

TCM has emerged as an effective alternative treatment for HCC patients with minimal side effects[29]. Several *in vivo* and *in vitro* experiments have shown that Chinese herbal formulas are based on invigorating qi, strengthening the spleen, tonifying the kidneys, and removing toxins and blood stasis. Therefore, TCM treatments considerably reduces proliferation, survival, and progression of HCC cells by regulating key signaling pathways such as PI3K/Akt, β-catenin, MAPK3, and RHOA[30-32]. SPXJ formula has been shown to stabilize tumors, improve patients' quality of life, and resist recurrence and metastasis in the clinical treatment of liver cancer[33,34]. In this study, we employed colony formation, wound healing, Transwell, and apoptosis assays to investigate the effects of the SPXJ formula on the HCC cells. The results demonstrated that the SPXJ formula effectively inhibited the proliferation, migration, and invasion of HCC cells. Moreover, the SPXJ formula significantly increased apoptosis of HCC cells. These results corroborated previous findings by our group[22]. Our experiments also demonstrated that the number of colonies were higher in the Chol group. This may be caused by cholesterol promoting lipid metabolism in the tumor cells and facilitating their proliferation[35-37].

Previous and current research into the mechanisms of tumor metastasis have focused on processes such as integrin-mediated cell adhesion, epithelial-mesenchymal transition, tumor angiogenesis, lymphangiogenesis, and the hypoxic microenvironment. However, the effects of mechanical forces on the tumor invasion of the extracellular matrix and tumor cell migration in the matrix are not well characterized. The biomechanical properties of cells influence cytoplasmic membrane fluidity, cell stiffness, adhesion, and structural composition of the cytoskeleton. Therefore, there is a greater need to investigate the mechanical aspects that influence tumor metastasis[38]. Cellular biomechanics is intricately linked with various cell behaviors, including division, differentiation, migration, and apoptosis. Cellular biomechanics plays a pivotal role in tumor metastasis. During the process of metastasis, tumor cells rely on movement and deformation for metastasis, invasion, and cell-cell adhesion. Therefore, understanding the biomechanics of these processes is crucial for gaining insights into the mechanisms underlying tumor metastasis and may also contribute to the development of targeted therapeutic strategies. Our data demonstrated that treatment with SPXJ-serum significantly inhibited migration of the HCC cells, with noticeable reduced rate of migration to the distant sites. Furthermore, treatment with SPXJ-serum reduced invasion of HCC cells into the Matrigel. This suggested that SPXJ may inhibit HCC cells from invading the stroma. The effects in HCC cells treated with SPXJ were similar to the effects observed in the MβCD-treated HCC cells. Conversely, HCC cells in the Chol group showed significantly higher migration and invasion abilities. These data were also in agreement with the morphological changes observed using the AFM. The SPXJ-treated HCC cells showed round morphology. Furthermore, increased cellular debris was observed in the culture medium of the SPXJ-treated HCC cells. In contrast, HCC cells in the MβCD group exhibited significantly elongated cell morphology and blurred edges. HCC cells in the Chol group did not show significant alterations in the cell morphology compared with the control group, except for the presence of slightly sharper edges.

The capacity of tumor cells to move and deform is associated with their mechanical properties. The stiffness of a tumor cell is a key feature that modulates essential functions such as cell division, differentiation, migration, and apoptosis. Cellular stiffness is associated with the cell membrane and subcellular components, including the cytoskeleton, nucleus, and other organelles. Therefore, understanding and characterizing these mechanical properties will provide valuable

insights into the behavior and functions of tumor cells. The cytoskeleton is primarily composed of microtubules, actin filaments, and intermediate fibers[39]. It represents the spatial architecture of a cell and acts as a connecting bridge between the cell and the external environment. The cytoskeleton plays a crucial role in facilitating cell migration and deformation[40]. Furthermore, the cytoskeleton contributes to overall plasticity of a cell[41]. Several studies have demonstrated a strong association between aberrant changes in cellular stiffness and cancer development[42]. Cancer cells exhibited significantly reduced elastic modulus values compared to the healthy cells[41]. The relative softness of the invasive tumor cells decreased their adhesion to the extracellular matrix and augmented their ability to detach from the primary tumor site. Young's modulus values are used to quantify cell stiffness, and indicate the extent of deformation in the tumor cells[38,43]. Lekka *et al*[44] performed AFM and reported that the reduced stiffness of highly invasive ovarian cancer cells (HeyA8) cells was associated with the remodeling of the actin cytoskeleton. Therefore, AFM was used in this study to determine changes in the stiffness of HCC cells. In comparison with the vehicle group, HCC cells in the SPXJ-serum group demonstrated regular cell surfaces without noticeable pores and higher Young's modulus values, both of which were indicative of increased cell stiffness. HCC cells in the M β CD group exhibited bright and regular cell areas. They also showed the highest Young's modulus values among different treatment groups. Conversely, HCC cells in the Chol group displayed blurred edges and pores. They also showed the lowest Young's modulus values among all treatment groups, thereby suggesting reduced cell stiffness.

In mammalian cells, cholesterol is a crucial component of the cell membranes[45,46], and constitutes up to 50% of the plasma membrane lipids[11]. It is involved in various cellular functions[46-49]. Cholesterol modulates membrane fluidity by modifying the permeability barrier properties of the lipid bilayers[50]. Cholesterol also regulates turgidity of the cell membrane[51] by influencing various physical mechanisms that are necessary for membrane homeostasis[52]. Several studies have suggested that cholesterol-rich membrane domains that are formed in the plasma membrane play a crucial role in regulating cellular stiffness. A previous study investigated how the biomechanical properties of cancer cells influence T-cell-mediated cytotoxicity and adoptive T-cell immunotherapy, and reported that malignant transformation and tumor progression was associated with the softening of the cancer cells. The plasma membranes of soft cancer cells are enriched in cholesterol. Therefore, stiffening of cancer cells by cholesterol depletion enhanced T-cell cytotoxicity and the efficacy of adoptive T-cells therapy against solid tumors in mice[10]. In the model membranes, cholesterol content influences fundamental mechanical parameters such as bending stiffness and modulus of elasticity[53] and the resistance of the membrane to stress-induced rupture such as increased line tension[53,54]. Biswas *et al*[55] demonstrated that cholesterol-depleted cells were prone to rupture because of increased membrane tension and its variability. In conjunction with the findings from previous studies, the regular cell morphology and increased invasive and migratory abilities of HCC cells in the Chol group may be linked to elevated cholesterol levels in the cell membrane facilitated by exogenous water-soluble cholesterol, thereby reducing cellular stiffness. Conversely, the diminished invasive and migratory abilities of HCC cells in the M β CD group may be attributed to the depletion of cholesterol levels in the cell membrane by M β CD. The effects of SPXJ formula on the HCC cells may also be attributed to changes in cholesterol levels in the cell membrane. This was verified by estimating cholesterol levels in the plasma membranes of HCC cells from distinct groups.

ACAT gene was first identified in 1993[56]. The ACAT gene family consists of ACAT1, ACAT2[57-59], and acyl-CoA: Diacylglycerol acyltransferase 1[60]. ACAT1 accounts for 80% of the total ACAT enzyme activity measured *in vitro*, and is expressed in many tissues and cell types, including hepatocytes and Kupffer cells of the liver, adrenal glands, neurons, and macrophages[61,62]. ACAT1 and ACAT2 are integral membrane proteins. ACAT1 and ACAT2 are not expressed simultaneously under physiological settings in the same cell type in any tissue[59,62]. As a cholesterol-metabolizing enzyme, ACAT1 forms cholesteryl esters by transferring long-chain fatty acids to cholesterol. We investigated whether the effects of the SPXJ formula on the stiffness of HCC cells were linked to changes in the ACAT1 protein expression levels. Western blotting experiments demonstrated that SPXJ-serum significantly increased ACAT1 protein expression levels compared to the vehicle group. Furthermore, depletion of cholesterol levels with M β CD or addition of exogenous cholesterol did not alter the protein expression levels of ACAT1. Previous studies have shown that the activity of ACAT2 was highly variable but the activity of ACAT was relatively constant[63].

The present study is a preliminary investigation into the role of SPXJ formula in altering cellular stiffness by regulating the expression levels of ATAC1 through *in vitro* experiments. It is not yet possible to attribute the role to any single component of SPXJ formula and the underlying molecular mechanisms are not yet clear. In the future, we plan to perform high-throughput screening and immunoprecipitation experiments to confirm the underlying mechanisms by which SPXJ formula modulates stiffness of tumor cells, including HCC.

CONCLUSION

In summary, our findings demonstrated that the SPXJ formula inhibited HCC invasion and metastasis by increasing ACAT1 protein expression levels and cellular stiffness by reducing cholesterol levels in the plasma membranes. This suggested that targeting the biomechanical properties of tumor cells is a promising and novel strategy for anti-tumor therapy. Our study provides valuable insights into the role of the SPXJ formula in HCC therapy. It represents an innovative treatment approach with significant potential to advance the field of oncology and improve the prognosis of HCC patients (Figure 8).

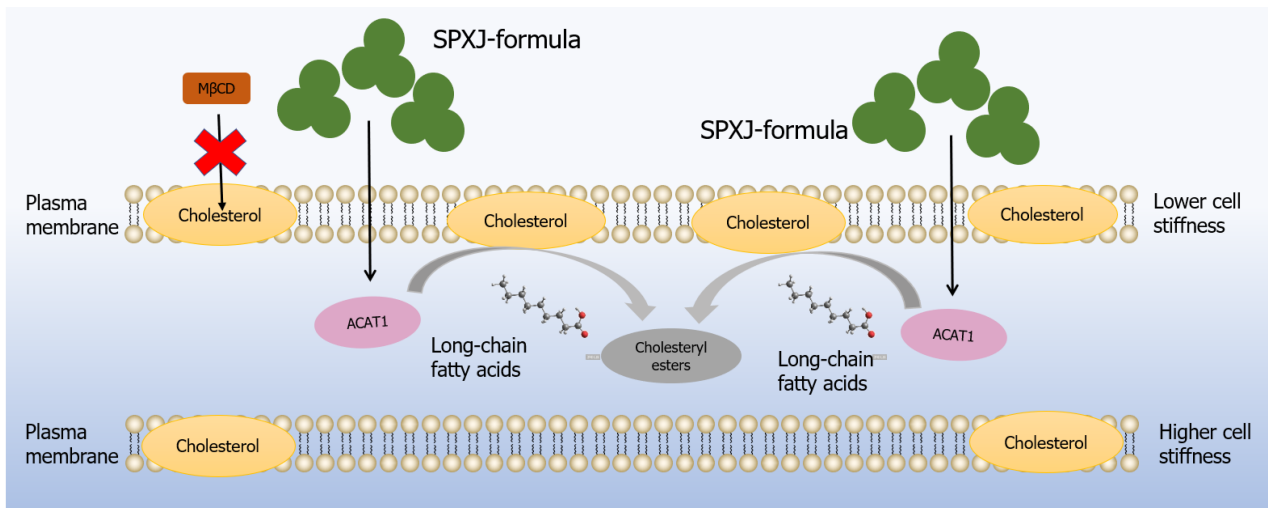


Figure 8 The effects of Shi-pi-xiao-ji-serum on cellular stiffness. SPXJ: Shi-pi-xiao-ji; MβCD: Methyl-β-cyclodextrin; ACAT1: Acetyl-coA acetyltransferase 1.

FOOTNOTES

Author contributions: Jian HY and Zhang Z designed the study; Jian HY and Liang ZC performed the experiments; Jian HY, Liang ZC, and Wen H collected and managed data; Jian HY analyzed data and visualized chart, and wrote the manuscript; Zeng PH and Zhang Z co-directed and supervised this manuscript, they are co-corresponding authors of this manuscript; and all authors approved the final version of the article.

Supported by the National Natural Science Foundation of China, No. 82074425; Hunan Science and Technology Planning Project, No. 2016SK2051 and No. 2023SK2057; and the Hunan Provincial Administration of Traditional Chinese Medicine Research Project, No. B2023089.

Institutional animal care and use committee statement: The animal study was approved by the Ethics Committee for Animal Research in Hunan University of Traditional Chinese Medicine (protocol code: LL2022070501).

Conflict-of-interest statement: All the authors report no relevant conflicts of interest for this article.

Data sharing statement: No additional data are available.

ARRIVE guidelines statement: The authors have read the ARRIVE guidelines, and the manuscript was prepared and revised according to the ARRIVE guidelines.

Open-Access: This article is an open-access article that was selected by an in-house editor and fully peer-reviewed by external reviewers. It is distributed in accordance with the Creative Commons Attribution NonCommercial (CC BY-NC 4.0) license, which permits others to distribute, remix, adapt, build upon this work non-commercially, and license their derivative works on different terms, provided the original work is properly cited and the use is non-commercial. See: <https://creativecommons.org/licenses/by-nc/4.0/>

Country of origin: China

ORCID number: Huan Wen 0000-0001-6056-6979; Zhen Zhang 0000-0001-9257-1449.

S-Editor: Wang JJ

L-Editor: A

P-Editor: Zhao S

REFERENCES

- 1 **Sung H**, Ferlay J, Siegel RL, Laversanne M, Soerjomataram I, Jemal A, Bray F. Global Cancer Statistics 2020: GLOBOCAN Estimates of Incidence and Mortality Worldwide for 36 Cancers in 185 Countries. *CA Cancer J Clin* 2021; **71**: 209-249 [PMID: 33538338 DOI: 10.3322/caac.21660]
- 2 **Yang R**, Gao W, Wang Z, Jian H, Peng L, Yu X, Xue P, Peng W, Li K, Zeng P. Polyphyllin I induced ferroptosis to suppress the progression of hepatocellular carcinoma through activation of the mitochondrial dysfunction via Nrf2/HO-1/GPX4 axis. *Phytomedicine* 2024; **122**: 155135 [PMID: 37856990 DOI: 10.1016/j.phymed.2023.155135]
- 3 **Chen W**, Zheng R, Zhang S, Zeng H, Xia C, Zuo T, Yang Z, Zou X, He J. Cancer incidence and mortality in China, 2013. *Cancer Lett* 2017;

- 401: 63-71 [PMID: 28476483 DOI: 10.1016/j.canlet.2017.04.024]
- 4 Llovet JM, Castet F, Heikenwalder M, Maini MK, Mazzaferro V, Pinato DJ, Pikarsky E, Zhu AX, Finn RS. Immunotherapies for hepatocellular carcinoma. *Nat Rev Clin Oncol* 2022; **19**: 151-172 [PMID: 34764464 DOI: 10.1038/s41571-021-00573-2]
 - 5 Chidambaranathan-Reghupaty S, Fisher PB, Sarkar D. Hepatocellular carcinoma (HCC): Epidemiology, etiology and molecular classification. *Adv Cancer Res* 2021; **149**: 1-61 [PMID: 33579421 DOI: 10.1016/bs.acr.2020.10.001]
 - 6 Liu CY, Chen KF, Chen PJ. Treatment of Liver Cancer. *Cold Spring Harb Perspect Med* 2015; **5**: a021535 [PMID: 26187874 DOI: 10.1101/cshperspect.a021535]
 - 7 Holenstein CN, Horvath A, Schär B, Schoenenberger AD, Bollhalder M, Goedecke N, Bartalena G, Otto O, Herbig M, Guck J, Müller DA, Snedeker JG, Silvan U. The relationship between metastatic potential and in vitro mechanical properties of osteosarcoma cells. *Mol Biol Cell* 2019; **30**: 887-898 [PMID: 30785850 DOI: 10.1091/mbc.E18-08-0545]
 - 8 Kita K, Asanuma K, Okamoto T, Kawamoto E, Nakamura K, Hagi T, Nakamura T, Shimaoka M, Sudo A. Cytoskeletal Actin Structure in Osteosarcoma Cells Determines Metastatic Phenotype via Regulating Cell Stiffness, Migration, and Transmigration. *Curr Issues Mol Biol* 2021; **43**: 1255-1266 [PMID: 34698103 DOI: 10.3390/cimb43030089]
 - 9 Molter CW, Muszynski EF, Tao Y, Trivedi T, Clouvel A, Ehrlicher AJ. Prostate cancer cells of increasing metastatic potential exhibit diverse contractile forces, cell stiffness, and motility in a microenvironment stiffness-dependent manner. *Front Cell Dev Biol* 2022; **10**: 932510 [PMID: 36200037 DOI: 10.3389/fcell.2022.932510]
 - 10 Lei K, Kurum A, Kaynak M, Bonati L, Han Y, Cencen V, Gao M, Xie YQ, Guo Y, Hannebelle MTM, Wu Y, Zhou G, Guo M, Fantner GE, Sakar MS, Tang L. Cancer-cell stiffening via cholesterol depletion enhances adoptive T-cell immunotherapy. *Nat Biomed Eng* 2021; **5**: 1411-1425 [PMID: 34873307 DOI: 10.1038/s41551-021-00826-6]
 - 11 Long T, Sun Y, Hassan A, Qi X, Li X. Structure of nevanimibe-bound tetrameric human ACAT1. *Nature* 2020; **581**: 339-343 [PMID: 32433613 DOI: 10.1038/s41586-020-2295-8]
 - 12 Han M, Hou JG, Dong CM, Li W, Yu HL, Zheng YN, Chen L. Isolation, synthesis and structures of ginsenoside derivatives and their anti-tumor bioactivity. *Molecules* 2010; **15**: 399-406 [PMID: 20110899 DOI: 10.3390/molecules15010399]
 - 13 Zhang S, Zhang M, Chen J, Zhao J, Su J, Zhang X. Ginsenoside Compound K Regulates HIF-1 α -Mediated Glycolysis Through Bclaf1 to Inhibit the Proliferation of Human Liver Cancer Cells. *Front Pharmacol* 2020; **11**: 583334 [PMID: 33363466 DOI: 10.3389/fphar.2020.583334]
 - 14 Jiao J, Yu J, Ji H, Liu A. Synthesis of macromolecular Astragalus polysaccharide-nano selenium complex and the inhibitory effects on HepG2 cells. *Int J Biol Macromol* 2022; **211**: 481-489 [PMID: 35584715 DOI: 10.1016/j.ijbiomac.2022.05.095]
 - 15 Ji H, Lou X, Jiao J, Li Y, Dai K, Jia X. Preliminary Structural Characterization of Selenium Nanoparticle Composites Modified by Astragalus Polysaccharide and the Cytotoxicity Mechanism on Liver Cancer Cells. *Molecules* 2023; **28** [PMID: 36838549 DOI: 10.3390/molecules28041561]
 - 16 Shao S, Duan W, Xu Q, Li X, Han L, Li W, Zhang D, Wang Z, Lei J. Curcumin Suppresses Hepatic Stellate Cell-Induced Hepatocarcinoma Angiogenesis and Invasion through Downregulating CTGF. *Oxid Med Cell Longev* 2019; **2019**: 8148510 [PMID: 30800209 DOI: 10.1155/2019/8148510]
 - 17 Deng Z, Xu XY, Yunita F, Zhou Q, Wu YR, Hu YX, Wang ZQ, Tian XF. Synergistic anti-liver cancer effects of curcumin and total ginsenosides. *World J Gastrointest Oncol* 2020; **12**: 1091-1103 [PMID: 33133379 DOI: 10.4251/wjgo.v12.i10.1091]
 - 18 Li W, Chen Y, He K, Cao T, Song D, Yang H, Li L, Lin J. The Apoptosis of Liver Cancer Cells Promoted by Curcumin/TPP-CZL Nanomicelles With Mitochondrial Targeting Function. *Front Bioeng Biotechnol* 2022; **10**: 804513 [PMID: 35242748 DOI: 10.3389/fbioe.2022.804513]
 - 19 Zeng P, Gao W, Pan M, Jiang Y, Li Y, Tang Z. [Prescription form of Strengthening Qi and Clearing Stasis and Poison effect on HepG2 liver cancer cell proliferation and the influence of the nude mouse transplantation tumor growth]. *Xiandai Zhongliu Yixue* 2014; **22**: 8-11 [DOI: 10.3969/j.issn.1672-4992.2014.01.03]
 - 20 Zeng P, Gao W, Pan M, Jiang Y, Li Y, Tang Z. [Effect of Prescription of Strengthening Qi and Clearing Poison and Toxin on Expressions of MVD, HIF1 α and VEGF/KDR from Hepg2 Hepatocellular Carcinoma Nude Mice Transplantation Tumor]. *Zhonghua Zhongyiyao Xuekan* 2014
 - 21 Zeng P, Gao W, Pan M, Jiang Y, Zhu K, Li Y, Liang H, Wang J, Tang Z. [Effect of Yiqi Huayu Jiedu Prescription on the Growth of HepG2 Nude Mice Transplantation Tumor and the Expression of Related Factors of Vascular Mimicry]. *Zhongguo Zhongyiyao Xinxi Zazhi* 2015; **22**: 55-59
 - 22 Yu S, Gao W, Zeng P, Chen C, Zhang Z, Liu Z, Liu J. Exploring the effect of Gupi Xiaoji Prescription on hepatitis B virus-related liver cancer through network pharmacology and in vitro experiments. *Biomed Pharmacother* 2021; **139**: 111612 [PMID: 33915505 DOI: 10.1016/j.biopha.2021.111612]
 - 23 Wei W, Wu XH, Li Y, Wei W, Wu XM, Li YJ. Experimental Methodology of Pharmacology. 4th ed. United States: ScienceOpen, 2010
 - 24 Yang W, Bai Y, Xiong Y, Zhang J, Chen S, Zheng X, Meng X, Li L, Wang J, Xu C, Yan C, Wang L, Chang CC, Chang TY, Zhang T, Zhou P, Song BL, Liu W, Sun SC, Liu X, Li BL. Potentiating the antitumor response of CD8(+) T cells by modulating cholesterol metabolism. *Nature* 2016; **531**: 651-655 [PMID: 26982734 DOI: 10.1038/nature17412]
 - 25 Brunt E, Aishima S, Clavien PA, Fowler K, Goodman Z, Gores G, Gouw A, Kagen A, Klimstra D, Komuta M, Kondo F, Miksad R, Nakano M, Nakanuma Y, Ng I, Paradis V, Nyun Park Y, Quaglia A, Roncalli M, Roskams T, Sakamoto M, Saxena R, Sempoux C, Sirlin C, Stueck A, Thung S, Tsui WMS, Wang XW, Wee A, Yano H, Yeh M, Zen Y, Zucman-Rossi J, Theise N. cHCC-CCA: Consensus terminology for primary liver carcinomas with both hepatocytic and cholangiocytic differentiation. *Hepatology* 2018; **68**: 113-126 [PMID: 29360137 DOI: 10.1002/hep.29789]
 - 26 Nagtegaal ID, Odze RD, Klimstra D, Paradis V, Rugge M, Schirmacher P, Washington KM, Carneiro F, Cree IA; WHO Classification of Tumours Editorial Board. The 2019 WHO classification of tumours of the digestive system. *Histopathology* 2020; **76**: 182-188 [PMID: 31433515 DOI: 10.1111/his.13975]
 - 27 Yang JD, Hainaut P, Gores GJ, Amadou A, Plymoth A, Roberts LR. A global view of hepatocellular carcinoma: trends, risk, prevention and management. *Nat Rev Gastroenterol Hepatol* 2019; **16**: 589-604 [PMID: 31439937 DOI: 10.1038/s41575-019-0186-y]
 - 28 Zheng R, Qu C, Zhang S, Zeng H, Sun K, Gu X, Xia C, Yang Z, Li H, Wei W, Chen W, He J. Liver cancer incidence and mortality in China: Temporal trends and projections to 2030. *Chin J Cancer Res* 2018; **30**: 571-579 [PMID: 30700925 DOI: 10.21147/j.issn.1000-9604.2018.06.01]
 - 29 Wang K, Chen Q, Shao Y, Yin S, Liu C, Liu Y, Wang R, Wang T, Qiu Y, Yu H. Anticancer activities of TCM and their active components

- against tumor metastasis. *Biomed Pharmacother* 2021; **133**: 111044 [PMID: 33378952 DOI: 10.1016/j.biopha.2020.111044]
- 30 **Wu Z**, Kang J, Tan W, Wei C, He L, Jiang X, Peng L. In Silico and In Vitro Studies on the Mechanisms of Chinese Medicine Formula (Yiqi Jianpi Jiedu Formula) in the Treatment of Hepatocellular Carcinoma. *Comput Math Methods Med* 2022; **2022**: 8669993 [PMID: 36345477 DOI: 10.1155/2022/8669993]
- 31 **Zhou Z**, Fu S, Li Y, Que Z, Liu X, Yu G, Gao D, Zhang Z, Wu T, Zhong Y. Molecular Mechanism of Bushen Jianpi Inhibition of Postoperative Recurrence and Metastasis of Hepatocellular Carcinoma. *J Biomed Nanotechnol* 2021; **17**: 53-63 [PMID: 33653496 DOI: 10.1166/jbn.2021.3018]
- 32 **Zhang C**, Xiang H, Wang J, Shao G, Ding P, Gao Y, Xu H, Ji G, Wu T. Exploring the mechanism of Jianpi Huatan recipe in protecting hepatocellular carcinoma based on network pharmacology. *J Ethnopharmacol* 2023; **317**: 116676 [PMID: 37279814 DOI: 10.1016/j.jep.2023.116676]
- 33 **Zhang Z**, Gao W, Wang Y, Li K, Zeng P. [Study on curative of Yiqi Huayu Jiedu decoction combined with solafenil in the treatment of primary hepatocellular carcinoma]. *Shaanxi Zhongyi* 2019; 322-324 [DOI: 10.3969/j.issn.1000-7369.2019.03.014]
- 34 **Zeng P**, Gao W, Pan M, Jiang Y, Cai M, Deng X, Chen M, Pan B, Li Y. [Clinical Study of the Law of Strengthening Qi and Clearing Stasis and Poison Combined Javanica Oil Emulsion Through Blood Vessels Involved in Treatment of Advanced Primary Liver Cancer]. *Liaoning Zhongyi Zazhi* 2013; **40**: 18-20
- 35 **Yang F**, Kou J, Liu Z, Li W, Du W. MYC Enhances Cholesterol Biosynthesis and Supports Cell Proliferation Through SQLE. *Front Cell Dev Biol* 2021; **9**: 655889 [PMID: 33791309 DOI: 10.3389/fcell.2021.655889]
- 36 **Chen Z**, Chen L, Sun B, Liu D, He Y, Qi L, Li G, Han Z, Zhan L, Zhang S, Zhu K, Luo Y, Zhang N, Guo H. LDLR inhibition promotes hepatocellular carcinoma proliferation and metastasis by elevating intracellular cholesterol synthesis through the MEK/ERK signaling pathway. *Mol Metab* 2021; **51**: 101230 [PMID: 33823318 DOI: 10.1016/j.molmet.2021.101230]
- 37 **Revilla G**, Pons MP, Baila-Rueda L, García-León A, Santos D, Cenarro A, Magalhaes M, Blanco RM, Moral A, Ignacio Pérez J, Sabé G, González C, Fuste V, Lerma E, Faria MDS, de Leiva A, Corcoy R, Carles Escollà-Gil J, Mato E. Cholesterol and 27-hydroxycholesterol promote thyroid carcinoma aggressiveness. *Sci Rep* 2019; **9**: 10260 [PMID: 31311983 DOI: 10.1038/s41598-019-46727-2]
- 38 **Smith PG**, Deng L, Fredberg JJ, Maksym GN. Mechanical strain increases cell stiffness through cytoskeletal filament reorganization. *Am J Physiol Lung Cell Mol Physiol* 2003; **285**: L456-L463 [PMID: 12704020 DOI: 10.1152/ajplung.00329.2002]
- 39 **Luo Q**, Kuang D, Zhang B, Song G. Cell stiffness determined by atomic force microscopy and its correlation with cell motility. *Biochim Biophys Acta* 2016; **1860**: 1953-1960 [PMID: 27288584 DOI: 10.1016/j.bbagen.2016.06.010]
- 40 **Fletcher DA**, Mullins RD. Cell mechanics and the cytoskeleton. *Nature* 2010; **463**: 485-492 [PMID: 20110992 DOI: 10.1038/nature08908]
- 41 **Grady ME**, Composto RJ, Eckmann DM. Cell elasticity with altered cytoskeletal architectures across multiple cell types. *J Mech Behav Biomed Mater* 2016; **61**: 197-207 [PMID: 26874250 DOI: 10.1016/j.jmbbm.2016.01.022]
- 42 **Bordeleau F**, Myrand Lapierre ME, Sheng Y, Marceau N. Keratin 8/18 regulation of cell stiffness-extracellular matrix interplay through modulation of Rho-mediated actin cytoskeleton dynamics. *PLoS One* 2012; **7**: e38780 [PMID: 22685604 DOI: 10.1371/journal.pone.0038780]
- 43 **Dallos P**, He DZ. Two models of outer hair cell stiffness and motility. *J Assoc Res Otolaryngol* 2000; **1**: 283-291 [PMID: 11547808 DOI: 10.1007/s101620010048]
- 44 **Lekka M**, Laidler P, Ignacak J, Łabedz M, Lekki J, Struszczyk H, Stachura Z, Hryniewicz AZ. The effect of chitosan on stiffness and glycolytic activity of human bladder cells. *Biochim Biophys Acta* 2001; **1540**: 127-136 [PMID: 11513974 DOI: 10.1016/s0167-4889(01)00125-2]
- 45 **Yeagle PL**. Cholesterol and the cell membrane. *Biochim Biophys Acta* 1985; **822**: 267-287 [PMID: 3904832 DOI: 10.1016/0304-4157(85)90011-5]
- 46 **Ikonen E**. Cellular cholesterol trafficking and compartmentalization. *Nat Rev Mol Cell Biol* 2008; **9**: 125-138 [PMID: 18216769 DOI: 10.1038/nrm2336]
- 47 **Byfield FJ**, Aranda-Espinoza H, Romanenko VG, Rothblat GH, Levitan I. Cholesterol depletion increases membrane stiffness of aortic endothelial cells. *Biophys J* 2004; **87**: 3336-3343 [PMID: 15347591 DOI: 10.1529/biophysj.104.040634]
- 48 **Goodwin JS**, Drake KR, Rimmert CL, Kenworthy AK. Ras diffusion is sensitive to plasma membrane viscosity. *Biophys J* 2005; **89**: 1398-1410 [PMID: 15923235 DOI: 10.1529/biophysj.104.055640]
- 49 **Shvartsman DE**, Gutman O, Tietz A, Henis YI. Cyclodextrins but not compactin inhibit the lateral diffusion of membrane proteins independent of cholesterol. *Traffic* 2006; **7**: 917-926 [PMID: 16787400 DOI: 10.1111/j.1600-0854.2006.00437.x]
- 50 **Al-Rekabi Z**, Contera S. Multifrequency AFM reveals lipid membrane mechanical properties and the effect of cholesterol in modulating viscoelasticity. *Proc Natl Acad Sci U S A* 2018; **115**: 2658-2663 [PMID: 29483271 DOI: 10.1073/pnas.1719065115]
- 51 **Morris CE**, Homann U. Cell surface area regulation and membrane tension. *J Membr Biol* 2001; **179**: 79-102 [PMID: 11220366 DOI: 10.1007/s002320010040]
- 52 **Kosmalska AJ**, Casares L, Elosgui-Artola A, Thottacherry JJ, Moreno-Vicente R, González-Tarragó V, Del Pozo MÁ, Mayor S, Arroyo M, Navajas D, Trepát X, Gauthier NC, Roca-Cusachs P. Physical principles of membrane remodelling during cell mechanoadaptation. *Nat Commun* 2015; **6**: 7292 [PMID: 26073653 DOI: 10.1038/ncomms8292]
- 53 **Needham D**, Nunn RS. Elastic deformation and failure of lipid bilayer membranes containing cholesterol. *Biophys J* 1990; **58**: 997-1009 [PMID: 2249000 DOI: 10.1016/S0006-3495(90)82444-9]
- 54 **Karatekin E**, Sandre O, Guitouni H, Borghi N, Puech PH, Brochard-Wyart F. Cascades of transient pores in giant vesicles: line tension and transport. *Biophys J* 2003; **84**: 1734-1749 [PMID: 12609875 DOI: 10.1016/S0006-3495(03)74981-9]
- 55 **Biswas A**, Kashyap P, Datta S, Sengupta T, Sinha B. Cholesterol Depletion by M β CD Enhances Cell Membrane Tension and Its Variations-Reducing Integrity. *Biophys J* 2019; **116**: 1456-1468 [PMID: 30979551 DOI: 10.1016/j.bpj.2019.03.016]
- 56 **Chang CC**, Huh HY, Cadigan KM, Chang TY. Molecular cloning and functional expression of human acyl-coenzyme A:cholesterol acyltransferase cDNA in mutant Chinese hamster ovary cells. *J Biol Chem* 1993; **268**: 20747-20755 [PMID: 8407899]
- 57 **Anderson RA**, Joyce C, Davis M, Reagan JW, Clark M, Shelness GS, Rudel LL. Identification of a form of acyl-CoA:cholesterol acyltransferase specific to liver and intestine in nonhuman primates. *J Biol Chem* 1998; **273**: 26747-26754 [PMID: 9756918 DOI: 10.1074/jbc.273.41.26747]
- 58 **Cases S**, Novak S, Zheng YW, Myers HM, Lear SR, Sande E, Welch CB, Lusis AJ, Spencer TA, Krause BR, Erickson SK, Farese RV Jr. ACAT-2, a second mammalian acyl-CoA:cholesterol acyltransferase. Its cloning, expression, and characterization. *J Biol Chem* 1998; **273**: 26755-26764 [PMID: 9756919 DOI: 10.1074/jbc.273.41.26755]
- 59 **Rogers MA**, Liu J, Song BL, Li BL, Chang CC, Chang TY. Acyl-CoA:cholesterol acyltransferases (ACATs/SOATs): Enzymes with multiple

- sterols as substrates and as activators. *J Steroid Biochem Mol Biol* 2015; **151**: 102-107 [PMID: 25218443 DOI: 10.1016/j.jsbmb.2014.09.008]
- 60 **Oelkers P**, Behari A, Cromley D, Billheimer JT, Sturley SL. Characterization of two human genes encoding acyl coenzyme A:cholesterol acyltransferase-related enzymes. *J Biol Chem* 1998; **273**: 26765-26771 [PMID: 9756920 DOI: 10.1074/jbc.273.41.26765]
- 61 **Chang CC**, Sakashita N, Ornvold K, Lee O, Chang ET, Dong R, Lin S, Lee CY, Strom SC, Kashyap R, Fung JJ, Farese RV Jr, Patoiseau JF, Delhon A, Chang TY. Immunological quantitation and localization of ACAT-1 and ACAT-2 in human liver and small intestine. *J Biol Chem* 2000; **275**: 28083-28092 [PMID: 10846185 DOI: 10.1074/jbc.M003927200]
- 62 **Chang TY**, Li BL, Chang CC, Urano Y. Acyl-coenzyme A:cholesterol acyltransferases. *Am J Physiol Endocrinol Metab* 2009; **297**: E1-E9 [PMID: 19141679 DOI: 10.1152/ajpendo.90926.2008]
- 63 **Parini P**, Davis M, Lada AT, Erickson SK, Wright TL, Gustafsson U, Sahlin S, Einarsson C, Eriksson M, Angelin B, Tomoda H, Omura S, Willingham MC, Rudel LL. ACAT2 is localized to hepatocytes and is the major cholesterol-esterifying enzyme in human liver. *Circulation* 2004; **110**: 2017-2023 [PMID: 15451793 DOI: 10.1161/01.CIR.0000143163.76212.0B]



Published by **Baishideng Publishing Group Inc**
7041 Koll Center Parkway, Suite 160, Pleasanton, CA 94566, USA
Telephone: +1-925-3991568
E-mail: office@baishideng.com
Help Desk: <https://www.f6publishing.com/helpdesk>
<https://www.wjgnet.com>

